International Journal of Refractory Metals and Hard Materials 95 (2021) 105448

Contents lists available at ScienceDirect

International Journal of Refractory Metals and Hard Materials

journal homepage: www.elsevier.com/locate/IJRMHM

First-principles investigation of W—V and W—Mo alloys as potential plasma facing materials (PFMs) for nuclear application

M.J. Phasha [a,*], A.S. Bolokang [b,c], M.A. Kebede [d]

[a] Transnet Engineering, Product Development, Private Bag X 528, Kilner Park, Pretoria 0127, South Africa
[b] Council for Scientific and Industrial Research, Manufacturing Cluster, Advanced Materials Engineering, Meiring Naudé Road, Brummeria, Pretoria 0185, South Africa
[c] Department of Physics, University of the Western Cape, Private Bag X 17, Bellville 7535, South Africa
[d] Council for Scientific and Industrial Research, Smart Places Cluster, Energy Centre, Meiring Naudé Road, Brummeria, Pretoria 0185, South Africa

ARTICLE INFO

Keywords:
Ab initio calculations
Virtual crystal approximation (VCA)
BCC W-V
BCC W-Mo
Solid solution
Phase stability
Elastic properties

ABSTRACT

Density-functional theory (DFT) based first-principles calculations were used to investigate the crystal structure, binding energy, phase stability and elastic properties of body-centered cubic (BCC) W-based binary solid solutions. The effect of alloying up to 50 atomic percent (at.%) concentration range is determined from the virtual-crystal approximation (VCA) approach. Resulting BCC solid solutions are assessed in comparison to the ideal Vegard's law. Solubility of the alloying elements is characterized by the negative enthalpy of mixing. The values of elastic constants computed for the ground state structures are used to assess the effect of alloying on the ductility and hardness. Based on current results, it seems key to strike a tricky balance between moderate Pugh's modulus ratio (B/G) between bulk and shear moduli (B,G) and elastic anisotropy (A) such that high hardness is not completely compromised at the expense of ductility. The predicted property trends are in agreement with existing theoretical and experimental data, which is indicative that the VCA approach is reliable in development of such alloys.

1. Introduction

Despite its key concerns such as environmental impact, safety and raw materials supply limitations, nuclear fusion still has a potential to become a source of safe and clean power generation, thus rendering nuclear power as a solution for future energy generation. However, with better selection of materials closer to the fusion reaction prone to becoming radioactive, such that they have short half-life, then the issue of disposing radioactive waste can be minimized or eliminated [1]. Plasma-facing materials (PFM) and plasma facing components (PFC) are exposed to the harsh nuclear fusion power plants environments as they act as the interface between the plasma and the material part [1,2]. Hence the operational conditions in such extreme environment require materials that can withstand high heat flux and surface neutron irradiation. Such a combination of demand poses a stiff challenge in terms of material performance. Consequently, great effort has been dedicated to search (theoretical and experimental) for suitable materials with high thermal conductivity, low sputtering yield and sufficient mechanical properties even under neutron irradiation. Due to their supreme high temperature properties such as high melting temperature, good thermal conductivity, high creep resistance, high temperature strength and good erosion resistance, tungsten (W) and tungsten based materials are found to be amongst the frontrunners as potential candidates for various fusion applications [2–4]. However, prior to application of such materials certain properties still need to be enhanced to improve their performance. The key properties that need to be improved are the low temperature ductility and fracture toughness as well as the ductile-to-brittle transition temperature (DBTT) while maintaining high temperature properties. One of the methods to improve the ductility and DBTT is through solid solution alloying. In many studies, the first-principles calculations have demonstrated the capability to investigate solid solution alloying in various systems [5–8] and was successful in predicting data that supported the existing experimental data.

Over the past decades, density functional theory (DFT) based methods have become a useful and viable tool to investigate behaviour of crystalline materials. These methods aid in facilitating the development of advanced materials by providing guidelines for design of new materials and give physical mechanistic insight into the origins of experimentally-derived trends. This is attributed to massive development efforts complemented by exponential increase in computational

* Corresponding author.
E-mail address: maje.phasha@gmail.com (M.J. Phasha).

https://doi.org/10.1016/j.ijrmhm.2020.105448
Received 28 October 2020; Received in revised form 18 November 2020; Accepted 22 November 2020
Available online 24 November 2020

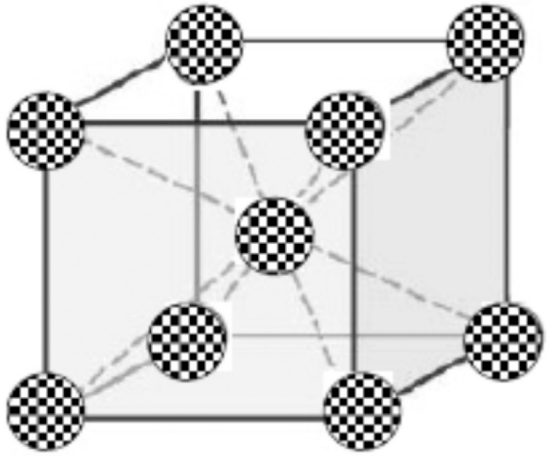

Fig. 1. Representation of BCC pseudo-binary solid solutions comprised of fractional composition $A_{1-x}B_x$.

power. Consequently, the DFT-based first-principles calculations have demonstrated the capability to generate results with high level of accuracy and comparable to experimental data [5–8]. The obtained materials data do not only provide insights about materials behaviour at electronic or atomic scale but can also be fed into a range of length and time scales modelling and simulation techniques capable of predicting materials performance at engineering scale. At this scale, the predictions of the macroscopic mechanical properties, such as flow stress, work hardening, and fatigue behaviour, in metals or other materials undergoing dislocation mediated plastic flow, is key [9].

In this study, a first-principles based virtual-crystal approximation (VCA) solid-solution unit-cell approach is used investigate the effect of alloying on various properties of W. It is well-known from metallurgy that solid-solution may have softening or hardening (strengthening) effect while in other systems induces phase transformation [5]. The W—V and W—Mo binary solid solution systems were chosen since they present 100% solubility [10,11], although in the current work the focus is limited to 50 at.% solute. A random solid solution (SS) with BCC crystal structure is represented by a model shown in Fig. 1. Ideally using this model, W-X (X = V, Mo) binary solid solution may be formed when an atom of W or X occupy randomly any position in the crystal, thus only changing the composition. In this manner, correct symmetry and crystal structure are maintained as they are both critical to predicting structural and elastic properties, with the latter linked to mechanical properties reported in experimental data. The composition can be varied by representing atoms as a fractional composition, $A_{1-x}B_x$. The details of the calculation for the elastic constants are presented in previous studies [5]. Unit cell approach allows for small composition variation W—V and W—Mo BCC SS. For further clarification, the full details of this method are described elsewhere [5]. Current approach differs slightly from earlier ab initio calculations studies conducted on similar materials in that supercell and ordered crystal structures were used [12].

2. Methodology

The ab initio modelling work was carried out using the CASTEP module within the Materials Studio software package [13]. The CASTEP code, a first principles quantum mechanical based programme for performing electronic structure calculations within the Hohenberg-Kohn-Sham density functional theory (DFT) [14,15], was used within the generalized gradient approximation (GGA) formalism [16] to describe the electronic exchange-correlation interactions. We used the recent Perdew-Burke-Ernzerhof (PBE) [17] form of GGA, which was designed to be more robust and accurate the density functional formalism and employs the plane-wave basis set to treat valence electrons and pseudopotentials to approximate the potential field of ion cores (including nuclei and tightly bond core electrons). Geometry optimization calculations were carried out maximum plane wave cut-off energy of 500 eV using robust Vanderbilt-type ultrasoft pseudopotentials (US) [18] and 16x16x16 Monkhorst-Pack [19] k-point mesh. Geometry optimization was conducted using the Broyden-Fletcher-Goldfarb-Shanno (BFGS) method [20]. We employed convergence criterion of less than 5×10^{-6} eV on total energy per atom, maximum displacement of 5×10^{-4} Å, residual forces of 3×10^{-2} eV $Å^{-1}$ and 2×10^{-2} GPa on the residual bulk stress. For each crystal structure, the geometry optimization was performed to obtain the equilibrium structural properties, from which the elastic constant were computed as described below. For each phase of interest, the geometry optimization is first performed to find its ground state, as well as to obtain the structural properties. W and Mo are isoelectronic with equal number of outer valence electrons while V is one electron less.

2.1. Phase stability

The cohesive (binding) energy of the pure elements and pseudo element or solid solution ($A_{1-x}B_x$) alloy was computed according to the relation

$$E_{Coh}^{A} = \frac{1}{n}E_{total}^{Solid} - E_{total}^{Atom} \quad (1)$$

where E_{total}^{Solid} is the total energy of the constituent element (A or B) or pseudo element ($A_{1-x}B_x$) in their ground-state crystal structures and E_{total}^{Atom} is the total energy of free atom (A or B) or pseudo-atom ($A_{1-x}B_x$), respectively. The fractions indicate the total number of atoms of constituent species in the unit cell, usually referred to as fractional composition. Energy of a free atom is calculated by creating a supercell (P1 symmetry) with lattice parameter a = 10 Å and placing an atom or pseudo atom at the center.

On the other hand, the enthalpy of mixing, H_{mix}, of the disordered solid solution is computed according to the relation:

$$H_{mix} = E_{Coh}^{A_{1-x}B_x} - \{(1-x)E_{Coh}^{A} + xE_{Coh}^{B}\} \quad (2)$$

where E_{Coh}^{A} and E_{Coh}^{B} are the cohesive energies of elemental A and B in their respective ground-state crystal structures. The fractional (atomic) composition of element A and B are represented by $(1 - x)$ and x, respectively.

2.2. Elasticity

The stress-strain relation may be used to distinguish the elastic and plastic regimes of solid materials [21]. The elastic moduli are the fundamental physical parameters which establish the stress-strain relation in the elastic regime. For an isotropic polycrystalline solid, the two independent elastic parameters are the bulk modulus (B) and the shear modulus (G). On the other hand, the resistance of solids to plastic or permanent deformation is governed by dislocation motion and may be expressed via the yield stress or mechanical hardness. The hardening mechanism in alloys, which arises from disturbances in the lattice caused by the solute atoms in the matrix, is often described by the classical Labusch-Nabarro model [22,23]. Furthermore, the ratio of B to G is used to describe the brittleness and ductility of metal with high (low) value corresponding to ductility (brittleness) of material [24]. Of great importance in metallurgical engineering design is how the solute atoms affect the elastic properties.

For each material, both stress and strain have three tensile and three shear components, giving six components in total. According to the theory of elasticity, 6 × 6 symmetry matrix with 36 elements is thus needed to describe the relationship between stress and strain. The structural symmetry of the crystal makes some of the matrix elements equal and others fixed at zero. For the cubic structures, only three elastic

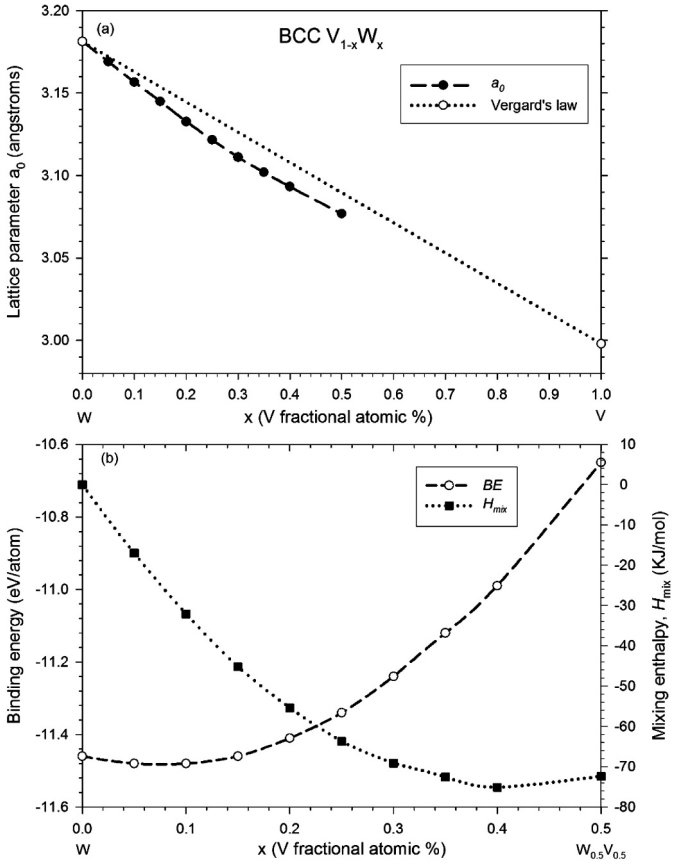

Fig. 2. Lattice parameter (a), binding energy and enthalpy of mixing (b) for BCC $W_{1-x}V_x$ ss plotted against V atomic composition.

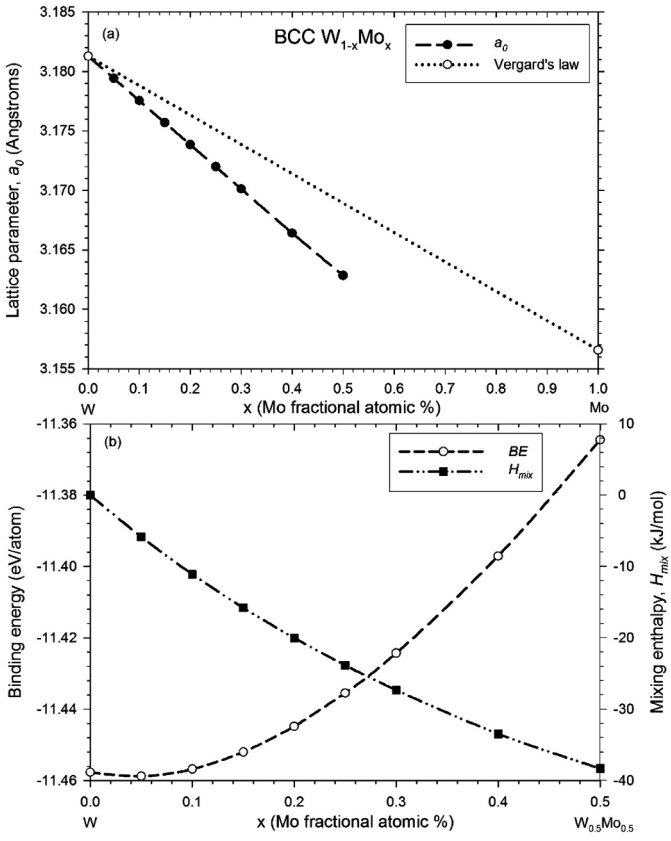

Fig. 3. Lattice parameter (a), binding energy and enthalpy of mixing (b) for BCC $W_{1-x}Mo_x$ ss plotted against Mo atomic composition.

constants, corresponding to C_{11}, C_{12}, and C_{44}, are independent. Appling two kinds of strains (ε_1 and ε_4) can give stresses relating to these three elastic coefficients, yielding an efficient method for obtaining elastic constants for the cubic system. This method has been successfully used to study the elastic properties of a range of materials including metallic systems [25]. The mechanical stability criteria of cubic systems as outlined elsewhere [26,27] are given as follows:

$$C_{44} > 0, C_{11} > |C_{12}| \; and \; C_{11} + 2C_{12} > 0 \tag{3}$$

Based on three independent single crystal elastic constants of a cubic crystal, C_{11}, C_{12}, C_{44}, the elastic moduli of polycrystalline material were calculated following averaging schemes of Voigt (upper bound) and Reuss (lower bound) by Hill (1952) as follows:

$$\begin{aligned} E &= \frac{9BG}{3B+G}; \nu = \frac{E}{2G-1}; G_V = \left[\frac{C_{11}-C_{12}+3C_{44}}{5}\right]; G_R \\ &= \left[\frac{5C_{44}(C_{11}-C_{12})}{4C_{44}+3(C_{11}-C_{12})}\right]; G_H = \left[\frac{G_V+G_R}{2}\right]; B = \left[\frac{C_{11}+2C_{12}}{3}\right]; C' \\ &= \frac{C_{11}-C_{12}}{2}; A = \frac{(2C_{44}+C_{12})}{C_{11}} \end{aligned} \tag{4}$$

where E is the modulus of elasticity, ν Poisson's ratio, G trigonal shear modulus, B bulk modulus, C' tetragonal shear modulus and anisotropic factor A. To predict for the first time the Vickers hardness of these systems from first-principles calculations, the model proposed by Chen et al. [28], as shown below, will be adopted as it relates the elastic moduli (B and G) with hardness.

$$H_v = 2\left(k^2 G\right)^{0.585} - 3 \tag{5}$$

where $k = \frac{G}{B}$ is the inverse Pugh's modulus ratio.

3. Results and discussion

3.1. Phase stability

As shown in Fig. 2(a), the lattice parameter decreases with increase in V composition as expected since the metallic atomic radius of V is smaller than that of W. However, this decrease in lattice parameter is linear but deviates negatively from the Vegard's rule shown by the dotted line. Nonetheless, the predicted trend as well as the negative deviation from Vegard's law are both in agreement with experimental observations [10]. In addition, the predicted lattice parameter of 3.181 Å for virgin W is also in agreement with existing experimental data. On the other hand, Fig. 2(b) indicates that the binding energy increases with V addition while the mixing enthalpy decreases, reaching a minimum at $W_{60}V_{40}$. Since the former is correlated to melting point, these results suggest decrease in melting temperature on alloying with V, in support of experimental data [10]. The enthalpy of mixing curve indicates that alloying with V is thermodynamically favourable with $W_{60}V_{40}$ composition being the most favourable. The minimum at this composition is in agreement with other theoretical results [4,29]. Similar trends as in Fig. 2 were obtained for BCC W—Mo system although the lattice parameter deviation from Vegard's law was more pronounced and enthalpy of mixing curve does not show any minima up to 50 at.% Mo, as shown in Fig. 3. This trend in H_{mix} could be attributed to isoelectronic behaviour of W and Mo.

3.2. Elasticity

Shown in Fig. 4(a) and (b) is the elastic constant and elastic moduli of BCC $W_{1-x}V_x$ ss plotted against V concentration while (c) presents the Pugh's modulus ratio as well as the anisotropy factor A. Of note is the distinct trends below and above 20 at.% V. With exception of elastic

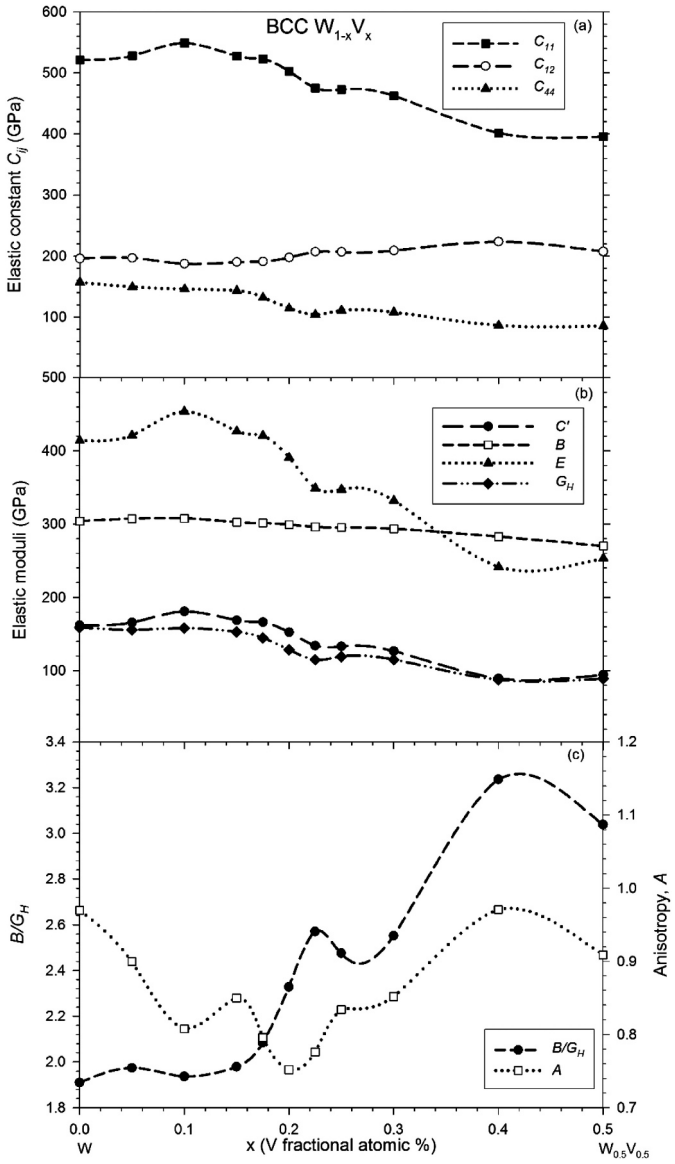

Fig. 4. Elastic properties of BCC $W_{1-x}V_x$ ss plotted against V atomic concentration.

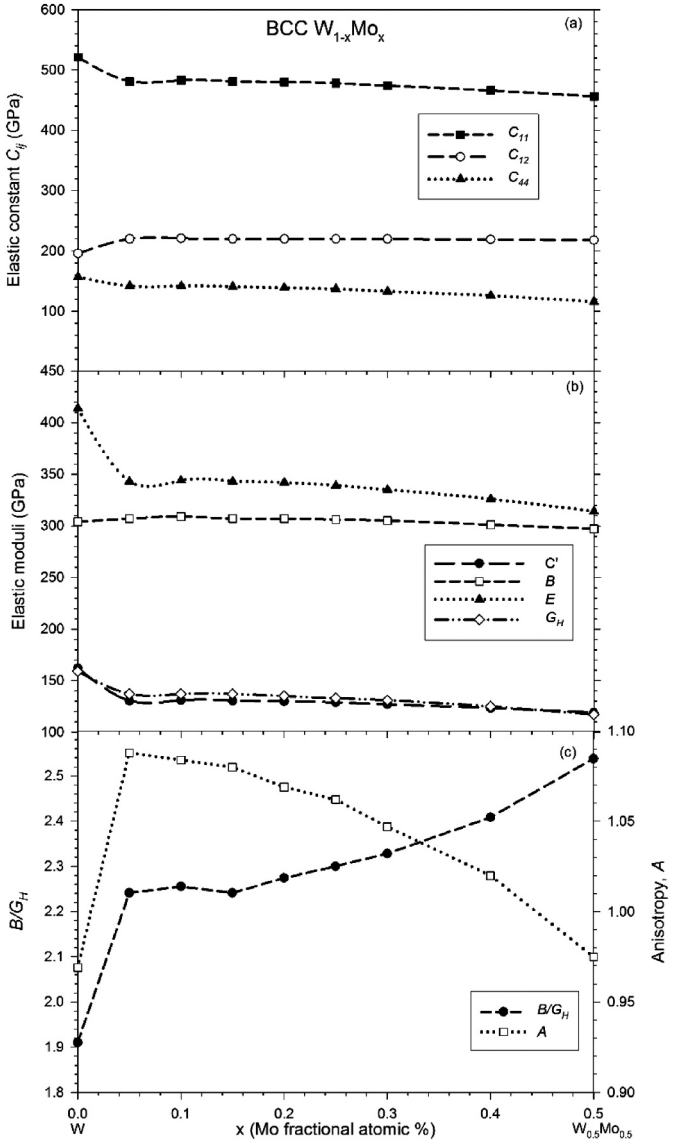

Fig. 5. Elastic properties of BCC $W_{1-x}Mo_x$ ss plotted against Mo atomic concentration.

constant C_{11}, other predicted elastic constants are almost constant below 20 at.% V, as shown in Fig. 4(a). This behaviour is followed by and either substantial increase or decrease beyond this composition. On the other hand, the trends for elastic moduli C', E and G_H shown in Fig. 4(b) follow a similar pattern while that of bulk modulus (B) is almost linear. The effects of the above mentioned changes become more meaningful when paying attention to Fig. 4(c) wherein all their individual behaviours are linked. It can be seen that Pugh's modulus ratio (B/G) slightly increases at smaller V content below 20 at.% and increase significantly at 20 at.% V and above. On the other hand, the behaviour of elastic anisotropy (A) is almost opposite that of B/G at compositions below 20 at.% but reaches minimum at 20 at.% and increases gradually thereafter. It worth noting that the B/G and A trends have maximum values at $W_{60}V_{40}$ which is the most thermodynamically favourable composition. Furthermore, all other elastic properties have minima at this composition, except for C_{12} which has maximum.

An anomalous behaviour when W is alloyed with small solute concentrations has been reported in the most promising PFM such as W—Re and W—Ir systems [2] and are correlated to significantly lower DBTT although the underlying fundamentals are not fully understood. Furthermore, more recently Arshad et al. reported from their experimental work that W—V alloys with lower V concentration (3.5 at.%) were highly damaged during transient heat loads while the intermediate V composition (16 at.%) performed comparatively better than both highest (28.5 at.%) and lowest V content alloys [30]. However, above 20 at.% V the materials becomes too ductile as indicated by rapid increase in Pugh's modulus ratio. A slightly different elastic behaviour is observed on BCC $W_{1-x}Mo_x$ system as shown in Fig. 5 below.

Despite a slight increase or decrease of individual elastic constants and their respective moduli upon addition of 5 at.% Mo, their trends almost flattens afterwards, as shown in Fig. 5(a) and 5(b), respectively. However, their combined effect on alloying is more pronounced in Fig. 5 (c) wherein the ductility of the solid solutions increase drastically at small composition of 5 at.% Mo and the increase becomes gradual afterwards. On the other hand, the elastic anisotropy (A) increases drastically at 5 at.% Mo and gradually decreases towards that of virgin W afterwards. In spite of a sudden rise in A upon introduction of Mo, the general trend is that elastic anisotropy decreases with increase in Mo. Nonetheless both systems considered in this study are thermodynamically favourable and mechanical stable at 0 K as indicated by negative enthalpy of mixing and $C' > 0$, respectively.

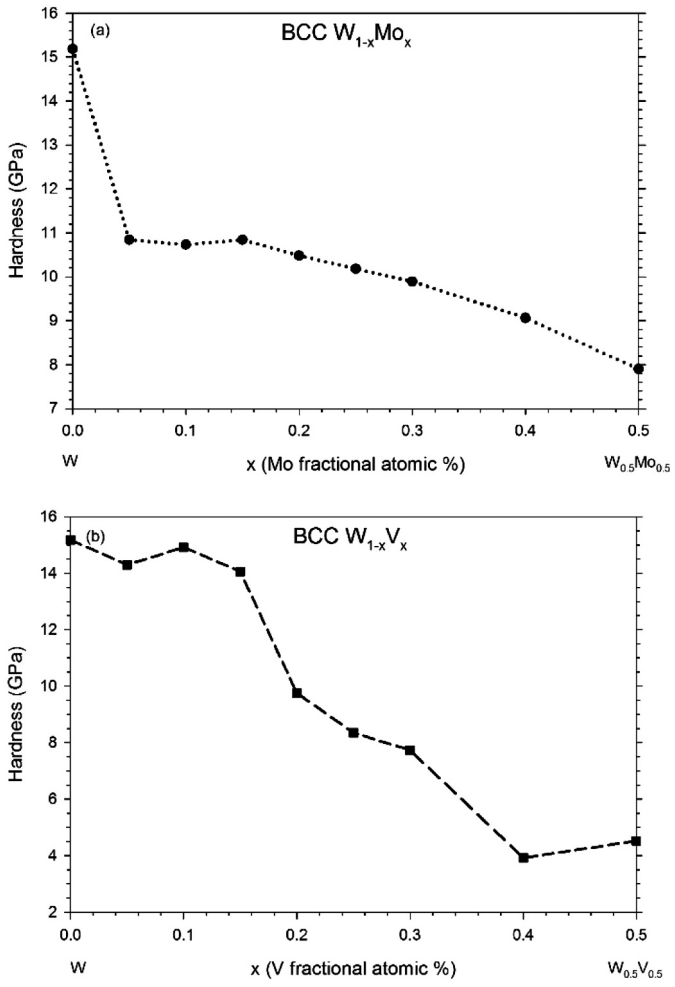

Fig. 6. Calculated Vickers Hardness of (a) BCC $W_{1-x}Mo_x$ and (b) $W_{1-x}V_x$ ss plotted against Mo and V atomic concentrations, respectively.

The calculated Vickers hardness (*Hv*) of both systems are shown in Fig. 6(a) and (b) for BCC $W_{1-x}Mo_x$ and $W_{1-x}V_x$, respectively. It is clear that the *Hv* trends correlate with elastic properties *E*, C_{44}, G_H and C' as they are linked by the relations in Eq. 4. This correlation is in agreement with earlier experimental study which made a correlation between hardness and C_{44} [31]. In addition, by virtue of Eq. 5, the *Hv* trends are opposite to Pugh's modulus ratio (*B/G*) trends due to their indirectly proportionality relation. It is evident from Fig. 6(a) that addition of small Mo significantly reduces the hardness of W although the decrease becomes gradual upon further alloying. This behaviour might render alloying with Mo undesirable for applications that require high hardness. However, the introduction of V up to 15 at.% composition seems to sustain high hardness complimented by slight increase in ductility but *A* is reduced, as shown in Fig. 6(b). The hardness drops significantly for V content above this composition as the material becomes too ductile. Unfortunately, according to authors knowledge, the experimental data on elastic or mechanical properties on these systems is not readily available to make direct comparison with our results. However, Arshad et al. [30] reported an increase in micro-hardness with up to 21 at.% V which is contrary to our hardness predictions. The discrepancy could stem from the fact the reported reduction in the crack density is not accounted for on the basis of increased ductility or toughness enhanced by alloying, properties which are well known to be indirectly proportional to hardness. Based on current results, it seems key to strike a tricky balance between moderate *B/G* and *A* such that high hardness is not completely compromised at the expense of ductility. In accordance with the above mentioned recent experimental findings, the present predictions prove to be useful in providing insight towards designing alloys with desired mechanical properties. Although the current results provide insight on how low temperature (0 K) brittleness in pure W can be overcome by alloying, it will be interesting to investigate in future the effects of lattice thermal vibrations at higher temperatures for the considered binary solid solutions. This is so because the effect of alloying on DBTT could be influenced partly by coefficient of thermal expansion. Moreover, it is known from thermodynamics that at higher temperatures the enthalpy of mixing and configurational entropy tends to further stabilize the solid solution.

4. Conclusion

Both systems considered in this study are thermodynamically favourable and mechanical stable at 0 K as characterized by negative mixing enthalpy and $C' > 0$. The Vickers hardness of BCC $W_{1-x}Mo_x$ and $W_{1-x}V_x$ solid solutions predicted for the first time using an ab initio technique are presented. Introduction of Mo significantly reduces the hardness of W while the introduction of up to 15 at.% V composition seems to sustain high hardness complimented by slight increase in ductility but *A* is reduced. Based on current results, it seems key to strike a tricky balance between moderate *B/G* and *A* such that high hardness is not completely compromised at the expense of ductility. In general, the predicted property trends are in agreement with existing theoretical and experimental data, which validates that the current unit-cell VCA approach is reliable in predicting structural and elastic properties of metallic solid solutions. The current results serve as a demonstration that VCA – based first-principles approach is a reliable tool that can be used to design and development of advanced materials such as W-based alloys with potential application in nuclear fusion reactors for future energy generation.

Declaration of Competing Interest

No conflict of interest exists.

Acknowledgements

The authors are grateful to the support of Department of Science and Innovation (DSI) through Center for High Performance Computing for their computational resources.

References

[1] D.M. Duffy, Fusion power: a challenge for materials science, Phil. Trans. R. Soc. A 368 (2010) 3315–3328.
[2] Rieth M. Linsmeier Ch, J. Aktaa, et al., Development of advanced high heat flux and plasma-facing materials, Nucl. Fusion 57 (2017), 092007.
[3] I. Smid, M. Akiba, G. Vieider, L. Plochl, Development of tungsten armor and bonding to copper for plasma-interactive components, J. Nucl. Mater. (258–63) (1998) 160–172.
[4] D. Nguyen-Manh, A.P. Horsfield, S.L. Dudarev, Self-interstitial atom defects in bcc transition metals: group-specific trends, Phys. Rev. B 73 (2006), 020101–4 (R).
[5] M.J. Phasha, P.E. Ngoepe, An alternative DFT-based model for calculating structural and elastic properties of random binary HCP, FCC and BCC alloys: Mg-Li system as test case, Intermetallics 21 (2012) 88–96.
[6] Y. Yamabe-Mitarai, T. Hara, M.J. Phasha, P.E. Ngoepe, H.K. Chikwanda, Phase transformation and crystal structure of IrTi, Intermetallics 31 (2012) 26–33.
[7] M.A. Kebede, M.J. Phasha, N. Kunjuzwa, M.K. Mathe, K.I. Ozoemena, Solution-combustion synthesized aluminium-doped spinel ($LiAl_xMn_{2-x}O_4$) as a high-performance lithium-ion battery cathode material, Appl. Phys. A Mater. Sci. Process. 121 (2015) 51–57.
[8] M.A. Kebede, M.J. Phasha, N. Kunjuzwa, L.J. le Roux, D. Mkhonto, K.I. Ozoemena, M.K. Mathe, Structural and electrochemical properties of aluminium doped $LiMn_2O_4$ cathode materials for Li battery: experimental and ab initio calculations, Sustain. Energy Technol. Assess. 5 (2014) 44–49.
[9] C. Varvenne, G.P.M. Leyson, M. Ghazisaeidi, W.A. Curtin, Solute strengthening in random alloys, Acta Mater. 124 (2017) 660–683.
[10] R. Kieffer, K. Sedlatschek, H. Braun, Tungsten alloys of high melting point, J. Less-Common Met. 1 (1959) 19–33.

[11] S.V. Nagender-Naidu, A.M. Sriramamurthy, P. Rama Rao, The Mo−W (molybdenum-tungsten) system, Bull. Alloy Phase Diagr. 5 (1984) 177–180.
[12] M. Muzyk, D. Nguyen-Manh, K.J. Kurzydlowski, N.L. Baluc, S.L. Dudarev, Phase stability, point defects, and elastic properties of W-V and W-Ta alloys, Phys. Rev. B 84 (2011), 104115.
[13] M.D. Segall, J.P.D. Lindan, M.J. Probert, C.J. Pickard, P.J. Hasnip, S.J. Clark, M. C. Payne, First principles simulation: ideas, illustrations and the CASTEP code, J. Phys. Condens. Matter 14 (2002) 2717–2744.
[14] P. Hohenberg, W. Kohn, Inhomogeneous electron gas, Phys. Rev. 136 (1964) B864–B871.
[15] W. Kohn, L.J. Sham, Self-consistent equations including exchange and correlation effects, Phys. Rev. 140 (1965) A1133–A1138.
[16] J.P. Perdew, Y. Wang, Accurate and simple analytic representation of the electron-gas correlation energy, Phys. Rev. B 45 (1992), 13244.
[17] J.P. Perdew, K. Burke, M. Ernzerhof, Generalized gradient approximation made simple, Phys. Rev. Lett. 77 (1996) 3865.
[18] D. Vanderbilt, Soft self-consistent pseudopotentials in a generalized eigenvalue formalism, Phys. Rev. B 7892 (R) (1990) 41.
[19] H.J. Monkhorst, J.D. Pack, Special points for Brillouin-zone integrations, Phys. Rev. B 13 (1976) 5188.
[20] T. Fischer, J. Almlof, General methods for geometry and wave function optimization, J. Phys. Chem. 96 (1992) 9768–9774.
[21] G. Ghosh, G.B. Olson, The isotropic shear modulus of multicomponent Fe-base solid solutions, Acta Mater. 50 (2002) 2655–2675.
[22] R. Labusch, Statistical theories of solid solution hardening, Acta Metall. 20 (1972) 917–927.
[23] F.R.N. Nabarro, The theory of solution hardening, Philos. Mag. 35 (1977) 613–622.
[24] S.F. Pugh, Relations between the elastic moduli and the plastic properties of polycrystalline pure metals, Philos. Mag. 45 (1954) 823–843.
[25] S. Kamran, K. Chen, L. Chen, Ab initio examination of ductility features of fcc metals, Phys. Rev. B 79 (2009), 024106.
[26] M.J. Mehl, B.M. Klein, D.A. Papaconstantopoulos, in: J.H. Westbrook, R. L. Fleischer (Eds.), Intermetallic Compounds: Vol. 1, Principles, John Wiley & Sons Ltd, 1994.
[27] J.F. Nye, Physical Properties of Crystals, Oxford University Press, Oxford, 1985.
[28] X.-Q. Chen, H. Niu, D. Li, Y. Li, Modeling hardness of polycrystalline materials and bulk metallic glasses, Intermetallics 19 (2011) 1275–1281.
[29] L. Gharaee, J. Marian, P. Erhart, The role of interstitial binding in radiation induced segregation in W-re alloys, J. Appl. Phys. 120 (2016), 025901.
[30] K. Arshad, D. Ding, J. Wang, Y. Yuan, Z. Wang, Y. Zhang, Z.-J. Zhou, X. Liu, G.-H. Lu, Surface cracking of tungsten-vanadium alloys under transient heat loads, Nucl. Mater. Energy 3-4 (2015) 32–36.
[31] J.S. Tse, Intrinsic hardness of crystalline solids, J. Super. Mater. 32 (2010) 177–191.